

# Electric Properties of AlGa<sub>N</sub>/Ga<sub>N</sub>/Si High Electron Mobility Transistors

H. Mosbahi

Universite de Sousse Institut Superieur du Transport et de la Logistique de Sousse

Malek GASSOUMI (✉ [malek.gassoumi@gmail.com](mailto:malek.gassoumi@gmail.com))

Institut National des Sciences Appliquees de Lyon

A. Bchetnia

Qassim University College of Science

M.A. Zaidi

Universite de Monastir Faculte des Sciences Economiques et de Gestion de Mahdia

---

## Research Article

**Keywords:** AlGa<sub>N</sub>/Ga<sub>N</sub>/Si HEMTs, electrical conductance, complex permittivity, modulus formalisms, strain relaxation.

**Posted Date:** September 27th, 2021

**DOI:** <https://doi.org/10.21203/rs.3.rs-917000/v1>

**License:** © ⓘ This work is licensed under a Creative Commons Attribution 4.0 International License.

[Read Full License](#)

---

# Abstract

This work investigated the electrical properties in AlGa<sub>N</sub>/Ga<sub>N</sub>/Si HEMTs grown by molecular beam epitaxy. The electrical behavior has been investigated using electric permittivity, modulus formalism and conductance measurements. As has been found from electrical conductance, dispersive behavior is related to barrier inhomogeneity and deep trap in barrier layer. On the other hand, the strain relaxation of charge transport is studied both permittivity and electric modulus formalisms.

## 1. Related Works

AlGa<sub>N</sub>/Ga<sub>N</sub> high electron mobility transistors have attracted a great deal of interest for biotechnical, biomedical, high-power and high-frequency applications [1–4]. Group III-nitride based materials are attractive due to their superior properties, such as, wide band gaps, large breakdown bias voltages, high conduction band offset, high thermal and chemical stability, strong spontaneous and piezoelectric polarization fields as well as an efficient carrier transport [5, 6]. A two-dimensional electron gas (2DEG) can occur, resulting from the latter feature, at the AlGa<sub>N</sub>/Ga<sub>N</sub> heterointerface and provides high sheet carrier concentrations [7, 8]. For instance, a high aluminium content is suitable in order to increase the electron confinement and polarization-induced charge densities [2]. In addition, the insertion of a thin spacer in a HEMT device is proved to increase the mobility of carriers and decreases the alloy scattering [9–11].

Defects, impurities, current collapse, hot electron effects and leakage current are, however, lead to a limitation of the device performances [12–15]. The hot electron effect reduced by AlN spacer. Also, the current collapse reduced by using insulated gate or by surface passivation [16–19]. On the other hand, doping deep acceptor atoms into the buffer layer makes the layer semi-insulating to decrease the leakage current [20,21]. However, the origin and location of the active traps were characterized by many techniques such as deep-level transient spectroscopy (DLTS) [8,22], conductance deep-level transient (CDLTS) [23,24] and capacitance-frequency-temperature mapping [25]. As has been really found, the conductance and capacitance of a device varied with the frequency of the applied alternating electric current [26]. This phenomenon is called capacitance and conductance dispersion and can cause a piezoelectric polarization strain relaxation model of AlGa<sub>N</sub>/Ga<sub>N</sub> Schottky diodes. In addition, the related conduction mechanism, the material quality and the trapping effects of the channel electron are investigated by low frequency noise measurement (LFN) [27–29]. Therefore, Hooge mobility fluctuations (HMF) and carrier number fluctuations (CNF) are two noise models, that can explained the LFN characteristics in AlGa<sub>N</sub>/Ga<sub>N</sub> HEMTs [30,31]. In the present work reports on a study of AlGa<sub>N</sub>/Ga<sub>N</sub>/Si HEMTs by dielectric characteristics. We have also investigated the electrical conductance, the dielectric formalism and the complex modulus. An attempt to correlate all of the results has been made in order to assign the contribution of different mechanisms to the conductance and relaxation processes.

## 2. Experiments

The AlGaIn/GaN HEMTs under investigation are grown on silicon (111) substrate by using molecular beam epitaxy (MBE). The active layers consist in a 500 nm thick of undoped AlN/AlGaIn buffer, a 1.8 μm undoped GaN channel, a 23 nm thick of undoped Al<sub>0.26</sub>Ga<sub>0.74</sub>N barrier and a 1 nm n<sup>+</sup>-GaN cap layer. The ohmic contact pads are patterned using e-beam lithography. Hereafter, the metallization by means of evaporated 12/200/40/100 nm Ti/Al/Ni/Au is deposited at 900°C during 30s. The Schottky gate is realized using 100/150 nm Mo/Au layers. On the other hand, the AlGaIn/GaN/Si HEMTs are passivated by 100/50 nm SiO<sub>2</sub>/SiN with N<sub>2</sub>O pretreatment. Dielectric properties were performed using a Keithley 236 source unit and conductance measurements were performed using a HP 4192 LF impedance analyzer at atmospheric pressure and room temperature.

### 3. Conductance Measurements

Conductance measurements have performed on AlGaIn/GaN HEMT at room temperature. Fig.1 shows the conductance as a function of radial frequency at different bias voltage V<sub>gs</sub>. It is found that the conductance characteristics remains constant at low frequencies and increase continuously at higher frequencies. As can be noticed, the conductance variation is composed of two regions. The direct conductance (G<sub>dc</sub>) shows the existence of a plateau at the lower frequency. In addition, at the higher frequency, the ac conductance obeys a power law feature. The conductance can be expressed as [32] :

$$G(\omega) = G_{dc} + G_{ac}(\omega) \quad (1)$$

with :

$$G_{ac}(\omega) \approx \omega^s$$

where G<sub>dc</sub> is the dc conductance,  $\omega$  is the angular frequency and s is the critical exponent. The critical exponent as illustrated in the inset of Fig.1. It can be seen that the critical exponent decreases going from 0.44 to 0.38. The reduction in critical exponent is assigned to structural defects, inhomogeneities of thickness and composition of the layer, inhomogeneous doping, non-uniformity of interfacial charges, interface roughness [33,34]. This proposal of explanation agrees will with the strain relaxation in the barrier layer, the barrier inhomogeneity and the particular distribution of the interface states at metal/semiconductor interface [26,35,36].

### 4. Dielectric Studies

The permittivity characteristics of the (Mo/Au)/AlGaIn/GaN heterointerface can be written as [37]:

$$\varepsilon_r = \varepsilon_r' - j \varepsilon_r'' \quad (2)$$

with :

$$\varepsilon_r' = \varepsilon_i + \frac{\varepsilon_s - \varepsilon_i}{1 + \omega^2 \tau^2}$$

and,

$$\varepsilon_r'' = \frac{\sigma}{\omega \varepsilon_0} + \frac{(\varepsilon_s - \varepsilon_i) \omega \tau}{1 + \omega^2 \tau^2}$$

where  $\varepsilon_r'$  and  $\varepsilon_r''$  are the real and imaginary parts of the complex relative permittivity respectively. Here  $\varepsilon_i$  is the relative permittivity,  $\varepsilon_s$  is the relaxation static relative permittivity,  $\omega$  is the angular frequency,  $\tau$  is the characteristics relaxation time,  $\varepsilon_0$  is the dielectric constant of

AlGaN and  $\sigma$  is the transport conductivity. Fig.2 shows the relative permittivity imaginary parts as a function of radial frequency. It is found that the relative permittivity imaginary parts decreases and remains constant at higher frequencies. However, the latter behavior is due to the dispersive behavior of the (Mo/Au)/AlGaN/GaN Schottky barrier diode. The dispersive behavior can be attributed to the strain relaxation in the AlGaN barrier layer under the (Mo/Au) Schottky gate [26,37,38]. It can be seen that the permittivity decreases with increasing frequency. It is worth noticing that the strain relaxation mechanism occurs to cause permittivity falls. In addition, the relaxation mechanism is expected to be a the enhanced collision between phonons and piezoelectric polarization dipoles [26].

Fig.3 shows the dielectric loss as a function of angular frequency at different bias voltage  $V_{gs}$ . It is found that the loss tangent decreases continuously with increases frequency. As also shown, at higher frequencies, the dielectric loss reaches constant values. At lower frequencies, the dielectric loss, however, rises sharply. The latter behavior is due to the relaxation mechanism and especially results from a decrease permittivity. The loss tangent have revealed a decreasing tendency according to the colossal dielectric response and the barrier inhomogeneity. At higher frequencies, the dielectric loss is enhanced due to piezoelectric polarization. More especially, the remains loss tangent is assigned to the occurrence of transport conductivity and energy is observed from the alternating field. This proposal of explanation agrees well with the strain relaxation in the barrier layer.

## 5. Complex Modulus Analysis

The complex electric modulus investigates the electrical transport in devices. In addition, the complex electric modulus provides an alternative approach based on the conductivity relaxation time and polarization analysis [39]. It is found that the complex electric modulus is related to the complex dielectric permittivity [40], it is given according to :

$$M^*(\omega) = \frac{1}{\epsilon_r(\omega)} = \frac{\epsilon_r' + j \epsilon_r''}{|\epsilon|^2} = M' + j M'' \quad (3)$$

where  $M'$  and  $M''$  are the real and imaginary electric modulus parts respectively.

Fig.4 shows the real part of electric modulus as a function of radial frequency. As can be noticed, the real part of electric modulus is very low at lower frequencies. The latter behavior is due to the absence of electrode processes and especially results from a long-range of the charge carriers in HEMT devices. At higher frequencies, the real part of electric modulus, however, exhibits a dispersion then tend towards  $M_\infty$  when the frequency rises. It is found that this continuous dispersion indicates that the electric conduction is due to the charge carriers mobility.

Fig.5 shows the imaginary part of electric modulus as a function of radial frequency. As can be noticed, the spectrum is composed of one asymmetric peaks at different bias voltage  $V_{gs}$ . It is worth noticing that these peaks represents of relaxation behavior nature. It is found that the dielectric relaxation is thermally carrier generation activated in AlGaN/GaN heterointerface. It can be seen that the low-frequency of the peak represents the frequencies range in which carrier generation (electrons or holes) moves over long distances. In addition, the high-frequency of the peak represents the frequencies range in which carrier generation is trapped in 2DEG. It is worth noticing that the existence of a inhomogeneous Schottky barrier heights mechanism for charge transport. However, emission current of electron, recombination current of holes and electrons, tunneling current and leakage current are the different current transport mechanisms in the Schottky barrier diodes [41-44]. On the other hand, the piezoelectric polarization nature of the strain relaxation mechanism is responsible for electrical conduction.

## 6. Summary

In the present work, we have investigated the electrical properties of (Mo/Au)/AlGaN/GaN/Si HEMTs. The conductance mechanism is characterized by using electrical conductance, while, relaxation phenomena is studied by using permittivity and modulus formalism. The electrical conductance measurement shows that the conductance processes are caused by the barrier inhomogeneity and the structural defects due to the strain relaxation mechanism. Thus, the frequency-dependent of permittivity and modulus response confirmed the strain relaxation due to the dispersive behavior of the Schottky gate.

## Declarations

### Contributions

1. H. MOSBAHI paper writing.
2. M. GASSOUMI- Data manipulation.
3. A. Bchetnia- Paper editing and English correction.

4. M. A. ZAID -Idea and concept.

### **Corresponding author**

Correspondence to M. GASSOUMI

**Code Availability** Not Applicable.

**Conflicts of Interest/Competing Interests** The authors have no conflicts of interest to declare that are relevant to the content of this article.

**Ethics Approval and Consent to Participate** All authors freely agreed and gave their consent for the publication of this paper.

**Acknowledgements and Funding;** Not Applicable

**Consent for Publication** All authors freely agreed and gave their consent for the publication of this paper

### **Declaration of Competing Interest**

The authors whose names are listed immediately below certify that they have NO affiliations with or involvement in any organization or entity with any financial interest (such as honoraria; educational grants; participation in speakers' bureaus; membership, employment, consultancies, stockownership, or other equity interest; and expert testimony or patent-licensing arrangements), or non-financial interest (such as personal or professional relationships, affiliations, knowledge or beliefs) in the subject matter or materials discussed in this manuscript.

## **References**

- [1] I. Cimalla, F. Will, K. Tonisch, M. Niebelschutz, V. Cimalla, V. Lebedev, G. Kittler, M. Himmerlich, S. Krischok, J. A. Schaefer, M. Gebinoga, A. Schober, T. Friedrich, and O. Ambacher, *Sens. Actuators B* 123, (2007) 740.
- [2] O. Ambacher, J. Smart, J. R. Shealy, N. G. Weimann, K. Chu, M. Murphy, W. J. Schaff, L. F. Eastman, R. Dimitrov, L. Wittmer, M. Stutzmann, W. Rieger, and J. Hilsenbeck, *J. Appl. Phys.* 85, 3222 (1999).
- [3] V. Kumar, A. Kuliev, R. Schwindt, M. Muir, G. Simin, J. Yang, M. A. Khan, I. Adesida, *Solid-State Electron.* 47, (2003) 1577.
- [4] M. J. Manfra, N. Weimann, Y. Baeyens, P. Roux, D. M. Tennant, *Electron. Lett.* 39, (2003) 694.

- [5] H. Morkoç, Handbook of Nitride Semiconductors and Devices, vol. I-III, Wiley-VCH, Berlin, 2008.
- [6] R. Dimitrov, L. Wittmer, H. P. Felsi, A. Mitchell, O. Ambacher, and M. Stutzmann, Phys. Status Solidi A168, (1998)R7.
- [7] M. Donahue, B. Lübbers, M. Kittler, P. Mai, and A. Schober, Appl. Phys. Lett. 102, (2013) 141607.
- [8] H. Mosbahi, M. Gassoumi, I. Saidi, H. Mejri, C. Gaquière, M.A. Zaidi, H. Maaref, Current Applied Physics. 13, (2013) 1359.
- [9] I.P. Smorchkova, L. Chen, T. Mates, L. Shen, S. Heikman, B. Moran, S. Keller, S.P. DenBaars, J.S. Spech, U.K. Mishra, J. Appl. Phys. 90, (2001) 5196.
- [10] Y. Cao, D. Jena, Appl. Phys. Lett. 90, (2007) 182112.
- [11] S.B. Lisesivdin, A. Yildiz, M. Kasap, Opt. Adv. Mater.-Rapid Commun. 1, (2007) 467.
- [12] R. Vetury, N. Q. Zhang, S. Keller, and U. K. Mishra, IEEE Trans. Electron Devices 48, (2001) 560.
- [13] Y.-R. Wu and J. Singh, J. Appl. Phys. 101, (2007) 113712.
- [14] C. Rivera and E. Munoz, Appl. Phys. Lett. 94, (2009) 053501.
- [15] G. Meneghesso, G. Verzellesi, R. Pierobon, F. Rampazzo, A. Chini, U. K. Mishra, C. Canali, and E. Zanoni, IEEE Trans. Electron Devices 51, (2004) 1554.
- [16] S. Arulkumaran, G. I. Ng, and Z. H. Liu, Appl. Phys. Lett. 90, (2007) 173504.
- [17] X. Hu, A. Koudymov, G. Simin, J. Yang, M. A. Khan, A. Tarakji, M. S. Shur, and R. Gaska, Appl. Phys. Lett. 79, (2001) 2832.
- [18] L. Shen, S. Heikman, B. Moran, R. Coffie, N.-Q. Zhang, D. Buttari, I. P. Smorchkova, S. Keller, S. P. DenBaars, and U. K. Mishra, IEEE Electron Device Lett. 22, (2001) 457.
- [19] L. Wang, W. D. Hu, X. S. Chen, and W. Lu, J. Appl. Phys. 108, (2010) 054501.

- [20] H.-S. Kang, C.-H. Won, Y.-J. Kim, D.-S. Kim, Y.J. Yoon, I.M. Kang, Y.S. Lee, J.-H. Lee, Phys. Status Solidi A 212, (2015) 1116.
- [21] J.-H. Lee, J.-M. Ju, G. Atmaca, J.-G. Kim, S.-H. Kang, Y.S. Lee, S.-H. Lee, J.-W. Lim, H.-S. Kwon, S.B. Lisesivdin, J.-H. Lee, J. Electron Devices Soc. 6, (2018) 1179.
- [22] T. Okino, M. Ochiai, Y. Ohno, S. Kishimoto, K. Maezawa and T. Mizutani, IEEE Electron Device Lett. 25,(2004) 523.
- [23] E. J. Miller, X. Z. Dang and H. H. Wieder, J. Appl. Phys. 87, (2000) 8070.
- [24] S. Quan, Y. Hao, and X. H. Ma, Chin. Phys. B 20,(2011) 018101.
- [25] H. Shih, M. Kudo and T. Suzuki, Appl. Phys. Lett. 101, (2012) 043501.
- [26] Y. Dawei, W.Fuxue, Z.Zhaomin, C. Jianmin and G.Xiaofeng, J. Semicond. 34, (2013) 014003-1.
- [27] M.E. Levinshstein, S.L. Rumyantsev, R. Gaska, J.W. Yang, M.S. Shur, Appl. Phys. Lett. 738, (1998) 1089.
- [28] A. Balandin, Electron. Lett. 36, (2000) 912.
- [29] S.A. Vitusevich, S.V. Danylyuk, N. Klein, M.V. Petrychuk, V.N. Sokolov, V.A. Kochelap, A.E. Belyaev, V. Tilak, J. Smart, A. Vertiatchikh, L.F. Eastman, Appl. Phys. Lett. 80, (2002) 2126.
- [30] A.L. McWhorter, Semiconductor Surface Physics, Univ. Pennsylvania Press, Philadelphia, PA, (1957), 207.
- [31] L.K.J. Vandamme, F.N. Hooge, IEEE Trans. Electron Devices 55, (2008) 3070.
- [32] A. K. Jonscher, Thin Solid Films 1, (1967) 213.
- [33] S. Zhu, R. L. Van Meirhaeghe, S. Forment, G. P. Ru, X. P. Qu and B. Z. Li, Solid-State Electron.48, (2004)1205.
- [34] Y. G. Chen, M. Ogura and H. Okushi, Appl. Phys. Lett. 82, (2003) 4367.

- [35] S. Zeyrek, Ş. Altındal, H. Yüzer, and M. M. Bülbül, *Appl. Surf. Sci.* 252, (2006) 2999.
- [36] Ş. Altındal, S. Karadeniz, N. Tuğluoğlu, and A. Tataroğlu, *Solid-State Electron.* 47, (2003) 1847.
- [37] B. I. Bleaney, B. Bleaney, *Electricity and magnetism*. 3rd ed. London: Oxford University Press, 1976.
- [38] F. S. Xue, *Research & Progress of SSE.* 27, (2007) 457.
- [39] S. EL. Kossi, F. I. H. Rhouma, J. Dhahri, K. Khirouni, *Physica B.* 440, (2014) 118.
- [40] C. Leon, P. Lunkenheimer, K.L. Ngai, *Phys. Rev. B.* 64, (2001) 184304.
- [41] S.M. Sze, *Physics of Semiconductor Devices*, second ed., Willey, New York, 1981.
- [42] D.W. Yan, D.J. Chen, R. Zhang, Y.D. Zheng, *Appl. Phys. Lett.* 96, (2010) 083504.
- [43] D. Donoval, M. Barus, M. Zdimal, *Solid State Electron.* 34, (1991) 1365.
- [44] F. Roccaforte, F. Giannazzo, F. Iucolano, J. Eriksson, M.H. Weng, V. Raineri, *Appl. Surf. Sci.* 256, (2010) 5727.

## Figures

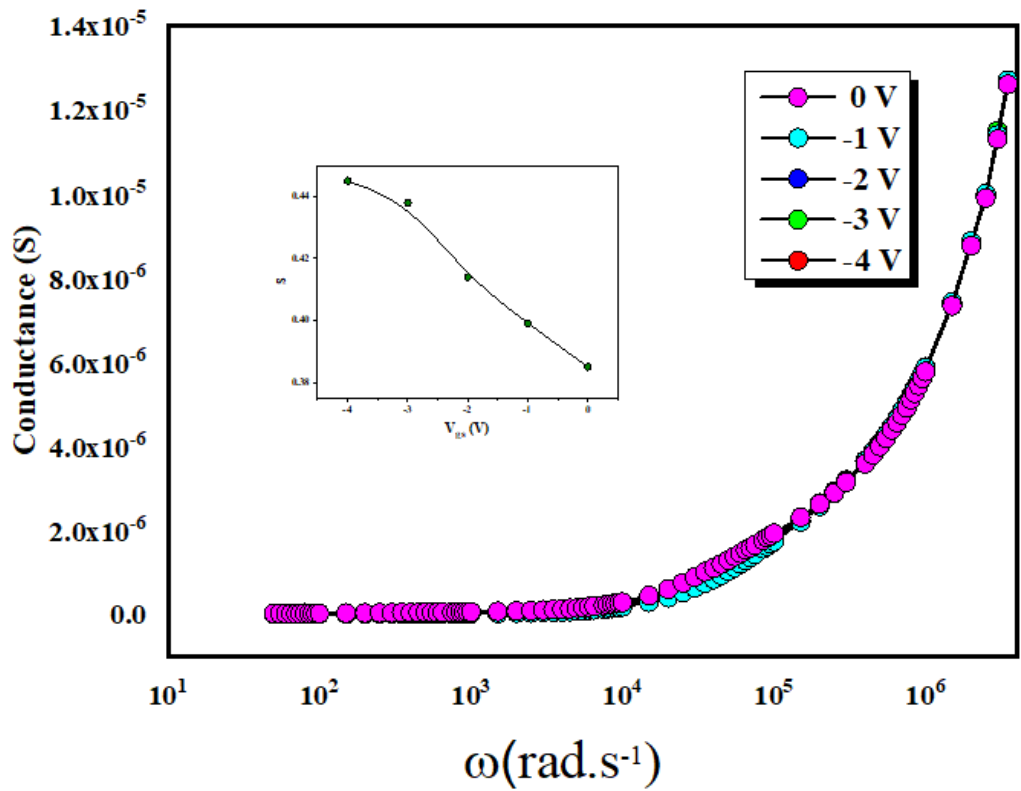


**Figure 1**

Frequency-dependent conductance of the AlGaN/GaN/Si HEMTs devices at different bias voltage. The inset represents the critical exponent, as determined from the linear fit of conductance characteristics.

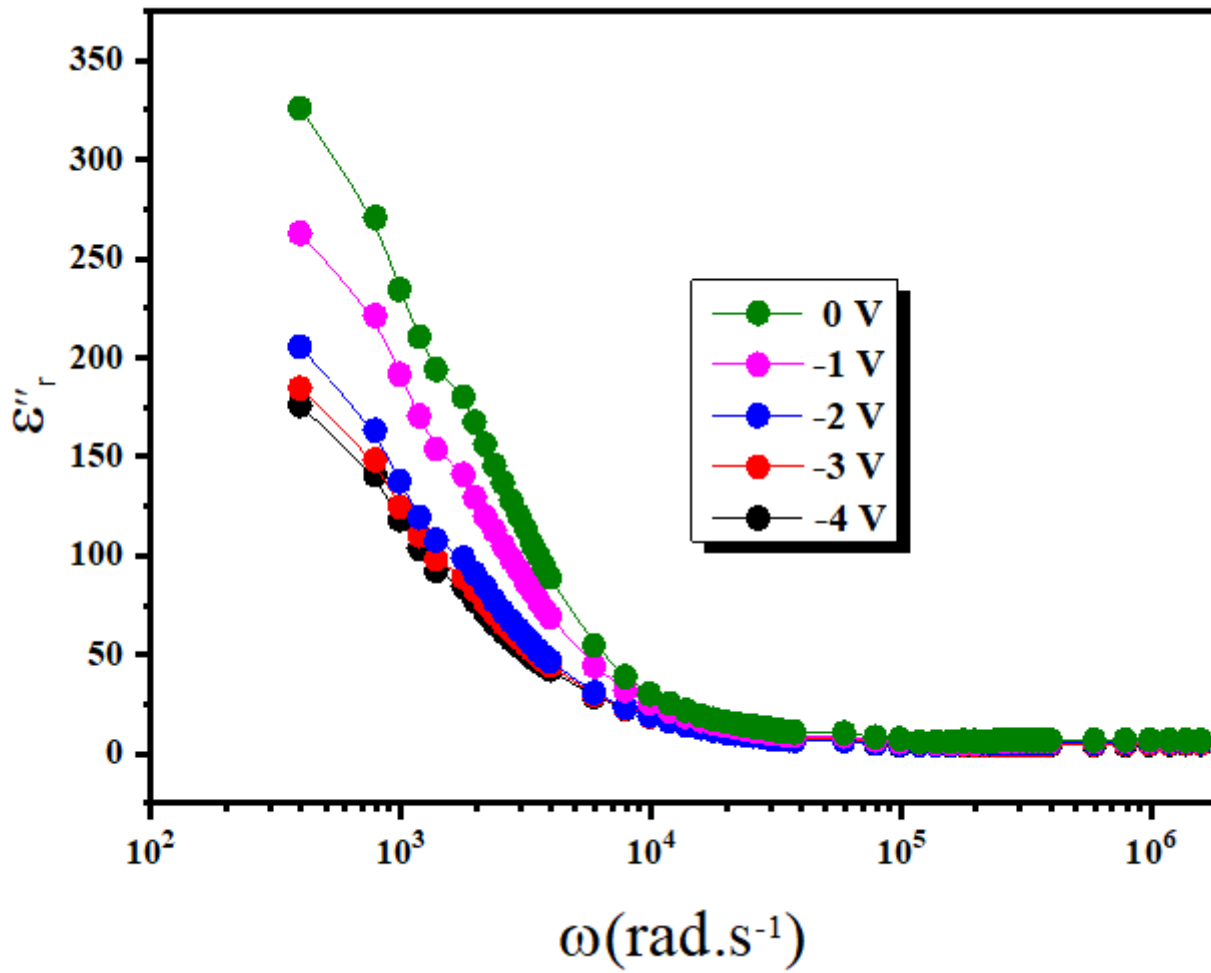


Figure 2

Frequency-dependent Dielectric constant of the AlGaIn/GaN/Si HEMTs at different bias voltage.

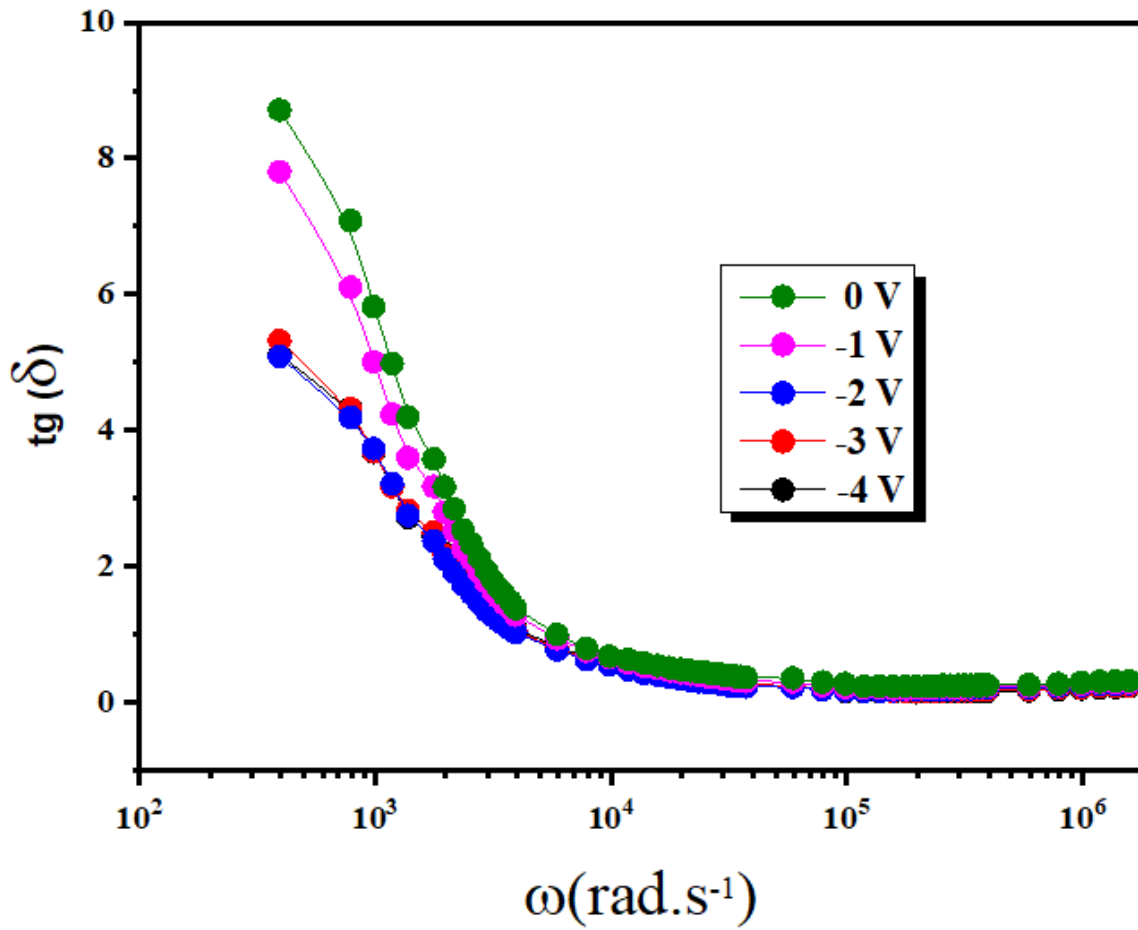


Figure 3

Dielectric loss ( $\tan \delta$ ) of the AlGaN/GaN/Si HEMTs devices at different bias voltage.

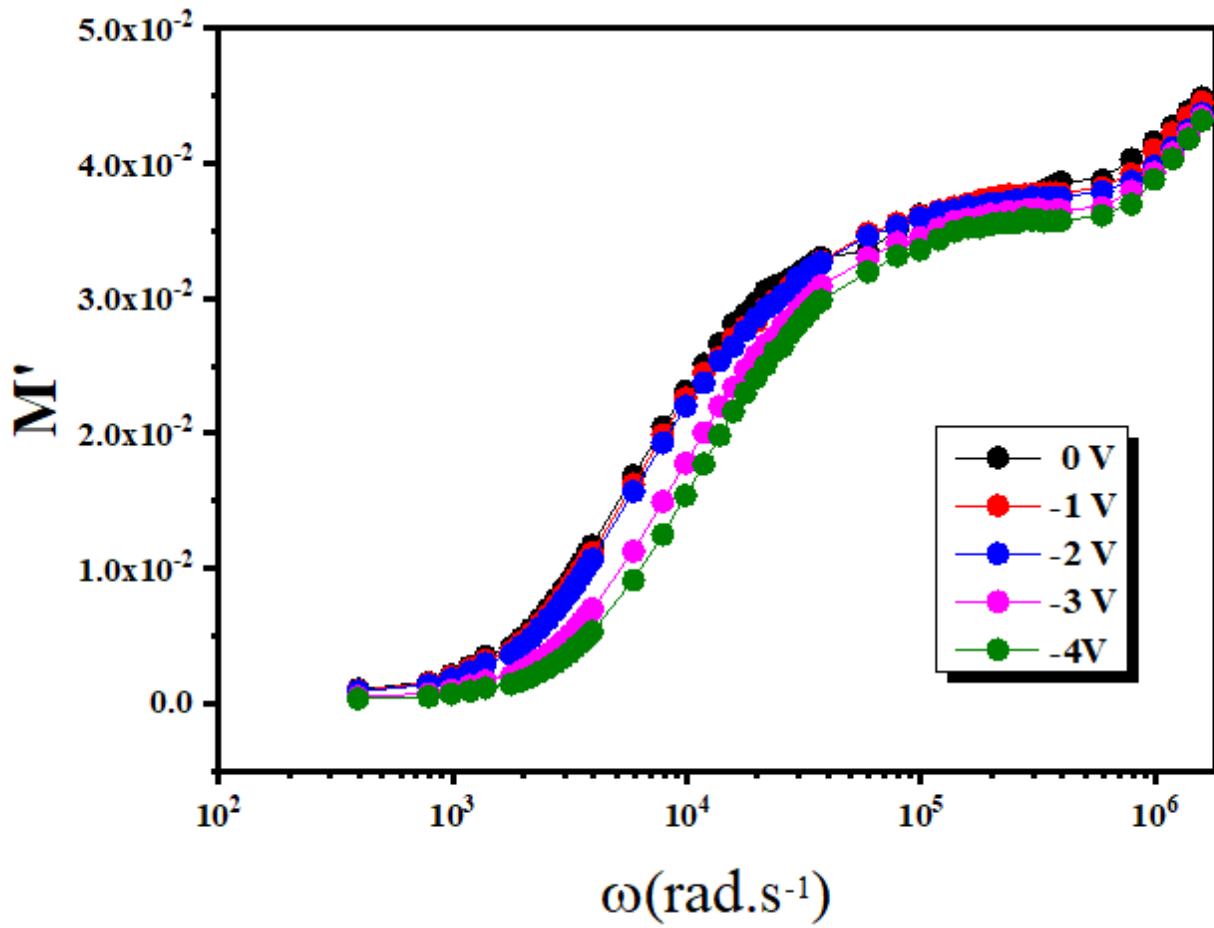


Figure 4

Real electric modulus of the AlGaIn/GaN/Si HEMTs devices at different bias voltage.

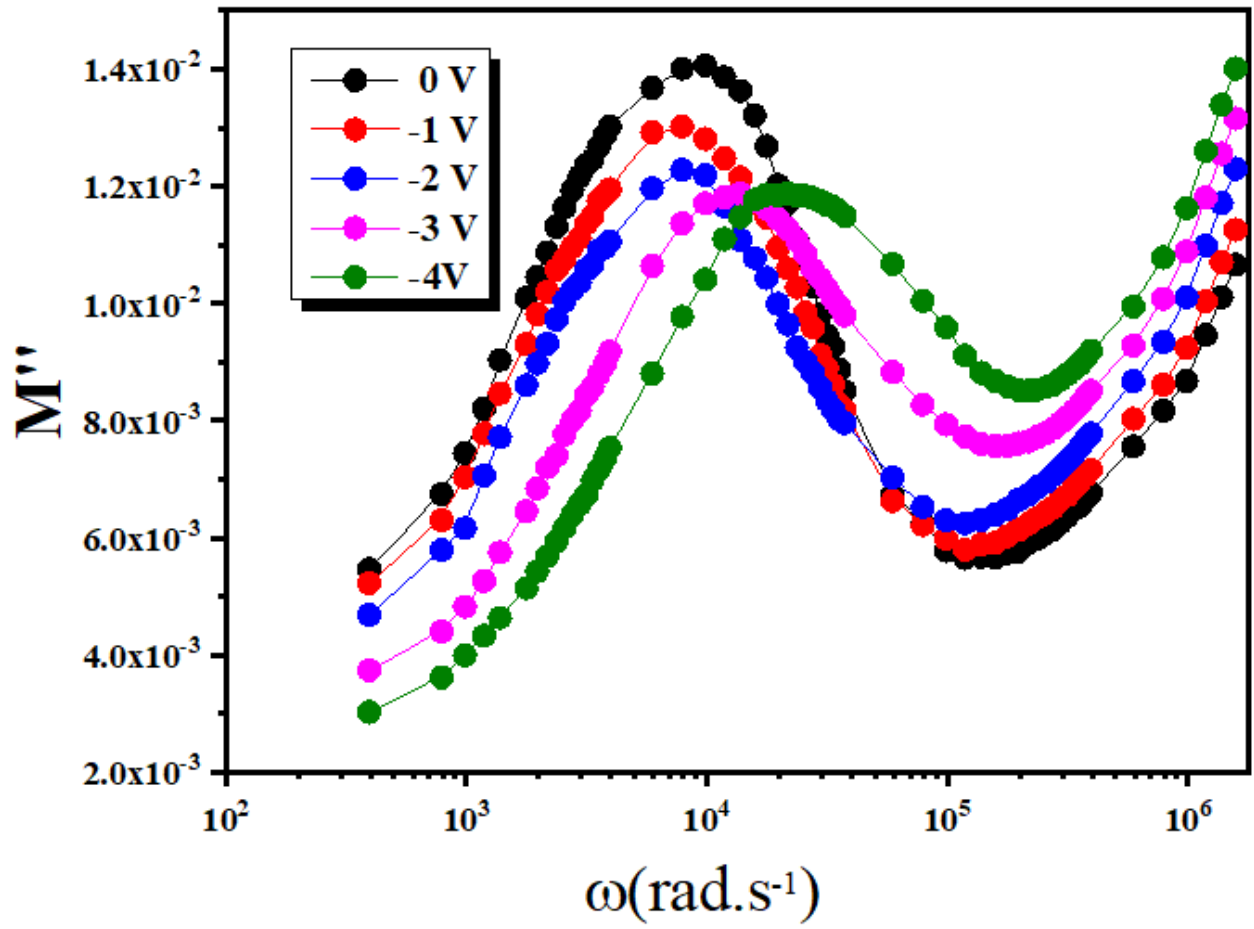


Figure 5

Imaginary electric modulus of the AlGaIn/GaN/Si HEMT devices at different bias voltage.